POLITECNICO DI TORINO
Repository ISTITUZIONALE

Voltage Divider Design for DC Traction in Tramway Networks

Original
Voltage Divider Design for DC Traction in Tramway Networks / Giordano, D., Letizia, P.S., Signorino, D., Colella, P., Pons, E., Waseem, M., Botondi, S., Trovato, V.. - ELETTRONICO. - (2025), pp. 1-5. (2025 IEEE International Conference on Environment and Electrical Engineering and 2025 IEEE Industrial and Commercial Power Systems Europe (EEEIC / I&CPS Europe) Chania, Crete, Greece 15-18 July 2025) [10.1109/eeeic/icpseurope64998.2025.11169159].

Availability:
This version is available at: 11583/3003543 since: 2025-10-01T10:05:54Z

Publisher:
IEEE

Published
DOI:10.1109/eeeic/icpseurope64998.2025.11169159

Terms of use:

This article is made available under terms and conditions as specified in the corresponding bibliographic description in the repository

Publisher copyright
IEEE postprint/Author's Accepted Manuscript

©2025 IEEE. Personal use of this material is permitted. Permission from IEEE must be obtained for all other uses, in any current or future media, including reprinting/republishing this material for advertising or promotional purposes, creating new collecting works, for resale or lists, or reuse of any copyrighted component of this work in other works.

(Article begins on next page)

14 September 2026

Voltage Divider Design for DC Traction in Tramway Networks

Domenico Giordano, Palma Sara Letizia, Davide Signorino
INRIM
Torino, Italy
d.giordano@inrim.it

Pietro Colella, Enrico Pons, Muhammad Waseem
Department of Energy "Galileo Ferraris"
Politecnico di Torino
Torino, Italy

Silvia Botondi, Vincenzo Trovato
Department of Civil, Environmental, Mechanical Engineering
Università di Trento
Trento, Italy

***Abstract*—This paper presents the study and development of a high-performance voltage transducer for the accurate monitoring and control of traction voltage in tramway systems. The proposed transducer offers a more effective alternative to the Hall-effect sensors currently adopted, which suffer from some drawbacks such as limited frequency bandwidth and unsuitability for outdoor applications. The research activity is carried out in different steps. Initially, the typical characteristics of the voltage signals to be monitored, such as amplitude dynamics and spectral content, are analyzed. Attention is then focused on the environmental conditions in which the monitoring voltage transducer must operate. These preliminary analyses allowed for the definition of the key design constraints for the sensor under study. The article describes the implementation of the voltage transducer, with particular focus on the transducer typology, components selection, and insulation techniques, tailored to the identified design constraints. Preliminary results from laboratory experimental tests are presented and discussed, demonstrating the voltage transducer's high performance, with amplitude linearity within tens of ppm from 50 V to 1 kV and a frequency response error lower than 0.15% up to 2 kHz.**

***Index Terms*—tramway system, voltage measurement, voltage divider, accuracy.**

I. Introduction

Urban tramway systems play a key role in the development of sustainable and efficient public transportation networks. Ensuring the reliability and safety of these systems depends heavily on accurate monitoring and control of the electrical power supply, particularly the traction voltage. Voltage transducers are critical components in this context, enabling real-time measurement and diagnostics essential for protective relaying, energy management, and system optimization. This paper analyses the commercial voltage sensors and presents the design and development of a high-performance voltage transducer specifically engineered for tramway applications. The proposed device is tailored to operate under harsh environmental conditions, including wide temperature ranges, mechanical vibrations, and strong electromagnetic interference, while maintaining high accuracy, long-term stability, and compliance with railway industry standards. The article discusses the design methodology, technological choices, and experimental validation of the prototype, highlighting its potential to enhance the safety and efficiency of modern light rail systems.

This study was carried out within the "DC smart grids for Next generation Transportation Systems" (NeTS) project – funded by European Union – Next Generation EU within the PRIN 2022 program (D.D. 104 - 02/02/2022 Ministero dell'Università e della Ricerca). This manuscript reflects only the authors' views and opinions and the Ministry cannot be considered responsible for them.

II. Limits of the commercial voltage sensors

Voltage measurement at the pantograph in rail and tramway transportation systems is commonly carried out using Hall effect transducers. The supply voltage of the rolling stock is converted into a current through a high-resistance resistor; this primary current generates a magnetic field within a magnetic core, which is then counterbalanced by a secondary current. The amplitude of this secondary current is regulated by a control system that ensures the magnetic flux within the core remains zero. In this way, the secondary current becomes proportional to the primary voltage. This method allows for the measurement of direct current (DC) signals while ensuring galvanic isolation. The main drawback of these sensors are as follows:

- The frequency bandwidth is typically limited to a few kilohertz (-3 dB).
- The sensor offset is temperature-dependent and often exhibits significant drift, which may necessitate periodic recalibration or replacement.
- The output is commonly provided as a current signal, requiring an additional current-to-voltage conversion stage.
- These sensors are generally designed for indoor applications.

III. Definition of design constraints

A. Characteristic of the voltage signal to measure

The voltage divider will be installed on trams powered by a 650 V DC supply system. The sensor's measurement dynamics should account for potential over-voltages that may occur during operation. This also enables the recording of power quality phenomena, such as voltage swells and fast transient overvoltages, for monitoring and predictive maintenance purposes. The measurement campaign conducted on board a 3 kV DC locomotive [1] as part of the MyRailS research project provided valuable statistical data on fast transient overvoltages recorded during normal service operations. Fig. 1 shows the overvoltage that occurs when the catenary is re-energized following the intervention of the substation's

main switchgear. The peak of the over-voltage is about double that of the rated voltage (3 kV). By rescaling the peak of the behaviour provided in Fig. 1, the maximum primary voltage which can be measured will be double of the rated one (V_r)

$$V'_{meas-max} = 2 \cdot V_r = 1300V \tag{1}$$

The divider shall have a withstand insulation voltage V_{ins} of 2 kV. Furthermore, since it will be placed outdoor, the air clearance between the high-voltage primary terminal and ground should exceed 20 cm, following the EN50191 standard.

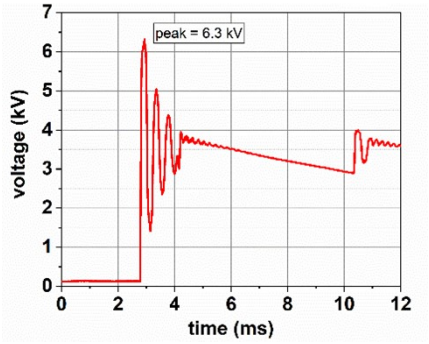

Fig. 1. Voltage transient behavior recorded at a pantograph of a DC traction unit after the re-energization of the catenary

B. Frequency range

As previously discussed, the divider is designed to provide a voltage signal serving a dual purpose: measuring power and monitoring power quality [2], specifically in terms of harmonic content and transient events. The theoretical harmonic content of the ripple produced by a 12-pulse diode rectifier converter is provided by the formula:

$$\begin{aligned} h &= k \cdot q_v; \qquad with\ k = 1, 2, 3, ... \\ a_k &= \cos(k\pi) \cdot \frac{2}{1 - k \cdot q_v} \end{aligned} \tag{2}$$

where h is the harmonic order of the power frequency, q_v is the pulsation index of the rectifier, and a_k is the relative amplitude of harmonic order h with respect to the amplitude of the DC voltage. Substations supplying DC transportation systems (railway, metro, tram) commonly include a second-order low-pass filter with a resonance frequency of 100 Hz. This filter dramatically reduces the harmonic content of the voltage ripple. A comparison between the harmonic content provided by a 12-pulse AC/DC converter, obtained by applying the 2 is provided in Fig. 2. The figure also shows (green line) the minimum relative amplitude of the harmonic, 0.001%, that can be reasonably detected; by a comparison between this limit and the filtered signal content, a maximum frequency amplitude that the divider shall transduce is f_{max}= 5 kHz. To limit the error introduced by the divider at this frequency, the -3 dB bandwidth should be at least 50% higher than f_{max}; therefore, the selected bandwidth is 7.5 kHz.

C. Target accuracy

The EN 50463-2 standard [3] provides a method for selecting the accuracy class of each component in the energy measurement chain, starting from the overall accuracy of the entire measurement chain ε_{EMF}. It is based on the following relationship:

$$\varepsilon_{EMF} = \sqrt{\varepsilon_{VMF}^2 + \varepsilon_{CMF}^2 + \varepsilon_{ECF}^2} \tag{3}$$

where ε_{VMF}, ε_{CMF} and ε_{ECF} are the accuracy class for the voltage sensor, the current sensor and the energy calculation unit. Assuming an overall accuracy of 1% for the energy measurement chain, an accuracy class of 0.5% for each of the three functions ensures that the total EMF error remains below the target threshold of 1 %.

D. Operating temperature range

The divider is intended for outdoor use. Considering harsh environmental conditions, the operating temperature range is set between -25°C and +50°C. Therefore, a temperature variation of -50°C to +25°C relative to the reference temperature of 25°C must be taken into account when estimating resistor variation due to environmental temperature changes.

E. Summary of the constraints

Based on the analysis presented in the previous section, the main constraints underlying the design of the divider are summarised in Table I.

TABLE I
DESIGN CONSTRAINTS

quantity	value
V_r	650 V
V_{ins}	2 kV
$V_{max-meas}$	1.3 kV
$V_{acq-max}$	100 V
Frequency bandwidth	7.5 kHz
Maximum dissipated Power	2 W
Minimum height HV terminal - ground	20 cm
Accuracy class	0.5 %
Operating temperature range	-25°C + 50 °C

IV. DESIGN OF THE VOLTAGE DIVIDER

A voltage divider is a passive Low Power Voltage Transformer (LPVT) consisting of a series connection of two impedances $\overline{Z}_{\mathrm{HV}}$ and $\overline{Z}_{\mathrm{LV}}$ [4]. Therefore, the voltage divider output signal $\overline{V}_{\mathrm{out}}$ can be easily obtained by leveraging Ohm's Law and Kirchhoff's Voltage and Current Laws as in the following (4):

$$\overline{V}_{\mathrm{out}} = \overline{V}_{\mathrm{in}} \cdot \frac{\overline{Z}_{\mathrm{LV}}}{\overline{Z}_{\mathrm{LV}} + \overline{Z}_{\mathrm{HV}}} \tag{4}$$

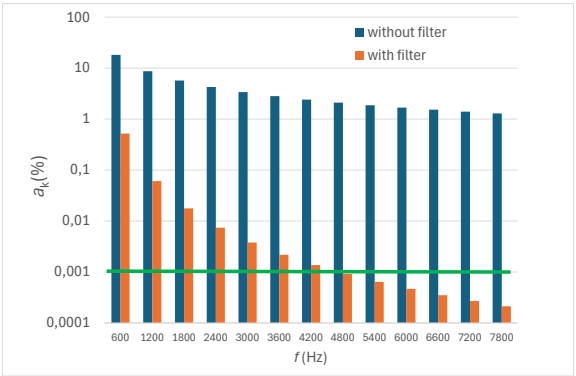

Fig. 2. Theoretical harmonic content for a 12-pulse AC-DC converter

Equation 4 shows that the output voltage is directly proportional to the input voltage and it can be suitably reduced by selecting the proper ratio k_r between the two impedances:

$$k_r = \frac{|\overline{V}_{\text{in}}|}{|\overline{V}_{\text{out}}|} = \frac{|\overline{Z}_{\text{LV}} + \overline{Z}_{\text{HV}}|}{|\overline{Z}_{\text{LV}}|} \tag{5}$$

A. Typology

Based on the nature of the impedances $\overline{Z}_{\text{HV}}$ and $\overline{Z}_{\text{LV}}$, three different types of voltage dividers can be identified as depicted in Fig 3: the impedance can be the series of resistors (resistive divider), capacitors (capacitive divider) or the parallel connection of resistors and capacitors (resistive-capacitive divider).

Based on their technologies, voltage dividers can have very different behaviour [5]. Capacitive dividers are unsuitable for DC or low-frequency measurements. Resistive dividers, on the other hand, are well-suited for DC and low-frequency voltages but offer a limited frequency bandwidth. Resistive-capacitive dividers cover a much broader frequency range, enabling voltage measurements from DC up to 10 MHz [6] [7]. However, they can be quite expensive, as their design requires considerable effort to minimise issues related to the transition between the resistive and capacitive behaviour of the divider [8] [9]. When the divider Scale Factor (SF) k_r (5) does not depend on the frequency of the input signal $\overline{V}_{\text{in}}$, the voltage divider is defined as compensated. This feature can be obtained i) by selecting the same component type for the high and low voltage branches and ii) by choosing the resistances R_{HV} and R_{LV} and the C_{HV} and C_{LV} capacitances according to the following (6):

$$R_{\text{HV}} \cdot C_{\text{HV}} = R_{\text{LV}} \cdot C_{\text{LV}} \tag{6}$$

Considering the frequency bandwidth to be analyzed (as reported in Table I), a resistive divider is implemented as a first attempt.

B. Selection of the resistive parameters

By the information provided in Table I, the rated divider SF k_r, defined as ratio between the rated output and rated input voltage (5), is fixed at 15 V/V. The maximum dissipated power of 1 W and the maximum permanent voltage $V_{max-meas}$ of 1.3 kV allow the determination of the high voltage resistance value:

$$R_{HV} \geq R_{HV_{max}} = \frac{V^2_{meas-max}}{P_{max}} = 0.845\ M\Omega \tag{7}$$

As a consequence, the low voltage resistance shall be:

$$R_{LV} \geq \frac{R_{HV_{max}}}{k_r - 1} \tag{8}$$

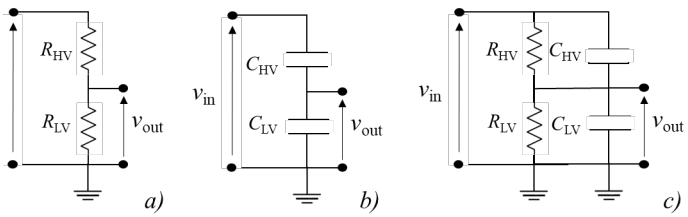

Fig. 3. Basic circuit representation of a) resistive, b) capacitive, and c) resistive-capacitive voltage divider.

TABLE II
HIGH VOLTAGE RESISTORS

quantity	value
Maximum power	2 W
Maximum operating voltage	10 kV
$\frac{\Delta R/R}{\Delta T}$	25 ppm/°C
$\frac{\Delta R/R}{\Delta V}$	-0.2 ppp/V

In order to control the frequency behaviour of the divider and the accuracy over the selected operating temperature and voltage range, the high voltage resistors shall be non-inductive with low temperature and voltage coefficients. Concerning the temperature and voltage coefficients for R_{HV}, it can be roughly estimated after this assumption, the estimated accuracy of the divider can be estimated by considering four sources: i) the temperature variation of the resistance value over the considered operating temperature range ε_{temp}, ii) the dependence of the resistance value to the applied voltage ε_{volt}, iii) the aging effect that affects the resistance value ε_{aging}, iv) the uncertainty associated with the measurement of the scale factor during the calibration ε_{cal}. Namely:

$$\varepsilon\% = \sqrt{\varepsilon^2_{temp} + \varepsilon^2_{volt} + \varepsilon^2_{aging} + \varepsilon^2_{cal}} \tag{9}$$

As a first attempt, all the source of uncertainty have the same value of 0.2%. This guarantees an overall uncertainty lower than the target value of 0.5%. With this assumption, it is possible to estimate the temperature coefficient $\frac{\Delta R/R}{\Delta T}$ for the resistors:

$$\frac{\Delta R/R}{\Delta T} = \frac{0.2}{75} = 0.0027\% \tag{10}$$

The same approach can be used to determine the voltage coefficient of the high-voltage resistors. Assuming a minimum voltage of 500 V and a maximum one of 780 V (120% of the rated supply voltage) the limits of the voltage dynamic in which the best measurement accuracy shall be guaranteed it is possible to estimate the voltage coefficient $\frac{\Delta R/R}{\Delta V}$:

$$\frac{\Delta R/R}{\Delta V} = \frac{0.2}{280} = 0.0007\% \tag{11}$$

At this point, all relevant information is available to proceed with the selection of the divider's resistors. The characteristics of the selected resistors for the high-voltage arm, which satisfy the design constraints described above, are summarized in Table II.

Since the operating voltage, 10 kV, is well below the maximum allowable value of 2 kV, it is possible to connect resistors in parallel to reach the designed resistance value ($R_{HV} \geq 0.875k\Omega$). Four 5 MΩ resistors are connected in parallel to reach a value of 1.24 $M\Omega$ to increase the total power dissipation capacity of the high-voltage resistor and to achieve an equivalent resistance close to the target value of $R_{HV} \geq 0.875$ MΩ. This configuration ensures that, at the maximum operating voltage of 1.3 kV, the power dissipated by each resistor, computed by 12, is well below the target dissipation power.

$$P_{max} = \frac{V^2_{max-meas}}{R_{HV}} \cdot \frac{1}{4} = 0.42W \tag{12}$$

The first trial value for the scale factor is provided by the relation:

$$k = \frac{V_{max-meas}}{V_{acq-meas}} = \frac{1300}{100} = 13\ V/V \tag{13}$$

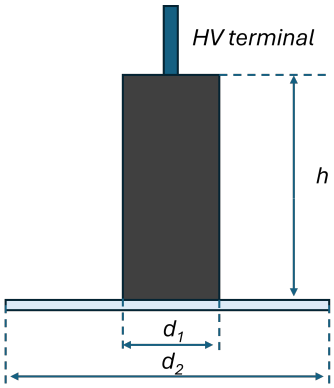

Fig. 4. Shape of the divider

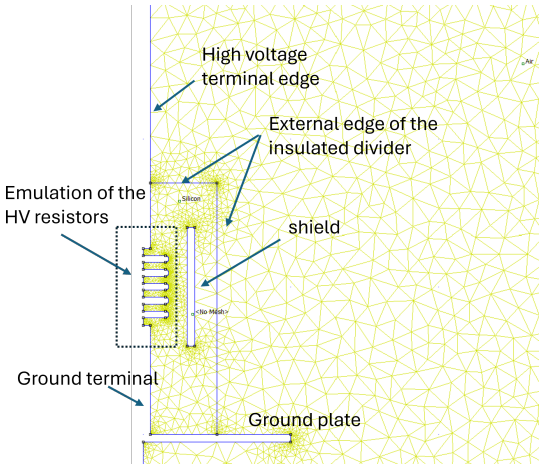

Fig. 5. Zoomed view of the axisymmetric model of the divider, highlighting the main components.

The rated scale factor shall be higher than the limit value computed in 13. After that, the low-voltage resistance can be computed, the first trial value is provided by the relation:

$$R_{LV} \geq \frac{R_{HV}}{k} = \frac{1.25 \cdot 10^6}{13} = 96\ k\Omega \qquad (14)$$

The low-voltage branch has been realised with a total resistance of 86 kΩ, obtained by connecting in series four 20 kΩ resistors and three 2 kΩ resistors.

C. Insulation design

The divider will be subjected to switching overvoltages and atmospheric impulses. Proper insulation design is essential to prevent partial or complete discharges, which—when triggered by overvoltages—can damage the device. To mitigate this risk, the electric field strength inside the divider must be limited under severe overvoltage conditions. This field strength strongly depends on the high-voltage configuration of the resistors, the presence of a shield that reduces capacitive coupling with the external environment, and the choice of insulation material.

The insulation design was carried out using FEMM software, which enables the computation of the electrostatic field in a 2D model. Moreover, it allows the determination of stray capacitive coupling, which can affect the frequency response of the divider.

Externally, the divider has a cylindrical shape, fixed at one end to a metal plate that enables mounting on the roof of the traction vehicle. The high-voltage terminal is located at the upper end of the cylinder. Figure 4 shows the shape of the divider. As a first design attempt, a height h of 17 cm and a diameter d_1 of 10 cm were chosen, with the plate diameter d_2 set to 20 cm. This structure has been modeled in FEMM CAD, as shown in Figure 5. A ground-connected shield has been added to reduce stray coupling between the high-voltage resistors and nearby conductive structures.

The four high-voltage resistors connected in parallel are modeled as a single element. To emulate the voltage gradient between the high-voltage terminal and ground, the resistor block is divided into five conductive segments, as shown in Fig. 5. Two different materials are present in the simulation: air medium outside the divider and silicon medium inside it, with a relative dielectric constant of 12. The electrostatic problem is solved by applying a 3 kV potential difference between the high-voltage terminal and ground. Each segment is assigned a voltage based on the relation $V_i = 3000 - 500 \cdot i$, where $i = 1, 2, ..., 5$ is the index of the resistor segment, with

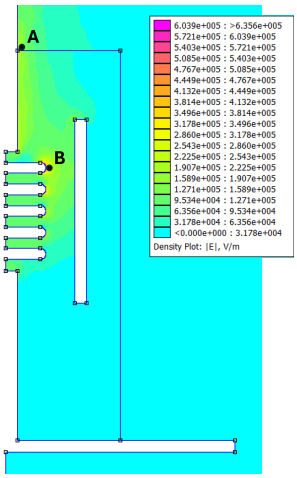

Fig. 6. Electric field intensity.

the first segment located at the top.

Fig. 6 shows the solution to the electrostatic problem as a chromatic map of the electric field strength. To demonstrate the effectiveness of the design, the electric field strength at two points was evaluated: point A, located on the top surface of the divider, and point B, on the surface of the first metallic cylinder emulating the high-voltage resistor. These values were then compared with the dielectric strength of air and silicone resin, respectively. Table III allows a comparison between the maximum electric strength and the dielectric strength for the two medium considered. One can conclude that the insulation is guaranteed at a supply voltage of 3 kV which is conservatively higher than the insulation one ($V_{ins}2\ kV$).

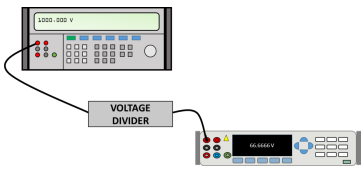

Fig. 7. Schematic rapresentation of the experimental setup adopted for the preliminary characterization of the voltege divider

TABLE III
FEMM RESULTS

point	simulation	medium	dielectric strenght at 20°C
point A	22 kV/cm	air	30 kV/cm
point B	52 kV/cm	silicon	650 kV/cm

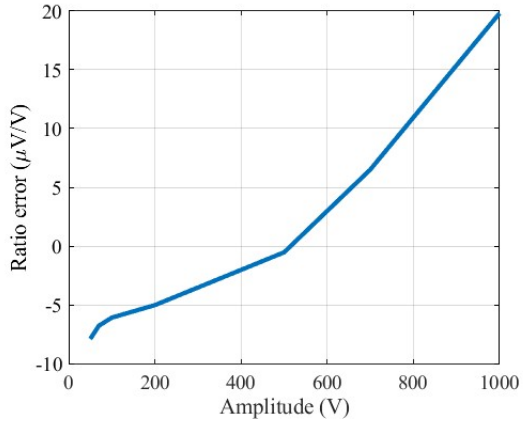

Fig. 8. DC characterization of the divider

V. Preliminary Voltage Divider Characterization

In this section, the experimental setup and procedure used to characterize the developed voltage divider are described. In particular, two distinct characterizations are carried out: the first evaluates the voltage divider dependence on the applied DC voltage, while the second investigates the frequency response of the voltage divider. For both the experimental test, the adopted setup is the one illustrated in Figure 7. DC and AC voltages are generated using a Fluke 5730A calibrator, while the output voltages of the voltage divider is measured with a Fluke 8588A digital multimeters. For each test point, the ratio error is evaluated according to the following (15):

$$\varepsilon = \frac{k_{\mathrm{n}} V_{\mathrm{s}} - V_{\mathrm{p}}}{V_{\mathrm{p}}} \tag{15}$$

where: k_{n} is the rated SF, whereas V_{p} and V_{s} are the acquired DC and AC values at the voltage divider primary and secondary sides, respectively.

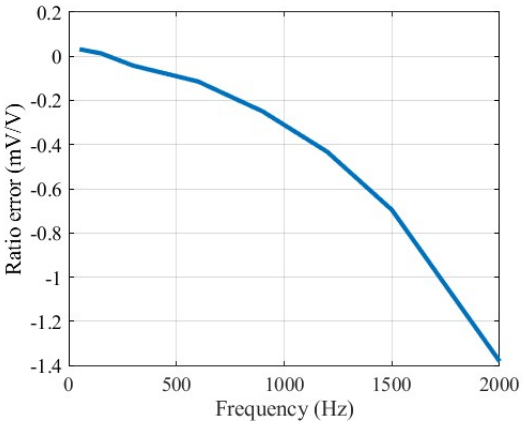

Fig. 9. Frequency response of the divider

Considering the DC voltage dependence test, the investigated range goes from 50 V to 1 kV and results are reported in Fig. 8. As can be observed, the divider is linear within tens of part per million (ppm).

As the frequency response, the voltage divider is supplied with an AC voltage at 200 V and frequency in [50 - 2k] Hz and results in term of ratio errors versus frequency are provided in Fig. 9. The realized divider exhibits a filtering behavior, as the error increases in absolute value with increasing frequency. However, within the investigated frequency range, the performance remains highly satisfactory, with a maximum error of -1.4‰ at 2 kHz.

Conclusion

The paper presents the design, implementation, and preliminary testing of a high-performance voltage divider specifically developed for DC tramway traction networks. The proposed voltage transducer addresses the limitations of commercial sensors, offering enhanced accuracy, a broader frequency response, and suitability for harsh outdoor environments.. It can measure up to 1.3 kV with 0.5% accuracy and works well in harsh outdoor conditions. Preliminary laboratory tests demonstrated excellent performance, showing amplitude linearity within tens of ppm across the full measurement range and frequency response errors below 0.15% up to 2 kHz. These results validate the design and highlight the potential of the proposed divider to improve safety and measurement reliability in modern tramway systems. Future work will focus on further experimental validation under real-world operational conditions and integration into full-scale traction monitoring systems.

References

[1] A. D. Femine, D. Gallo, D. Giordano, C. Landi, M. Luiso, and D. Signorino, "Power quality assessment in railway traction supply systems," *IEEE Transactions on Instrumentation and Measurement*, vol. 69, no. 5, pp. 2355–2366, 2020.

[2] D. Giordano, D. Signorino, A. D. Femine, D. Gallo, and G. Cipolletta, "Power quality in dc railway systems," in *2021 IEEE 11th International Workshop on Applied Measurements for Power Systems (AMPS)*, 2021, pp. 1–6.

[3] "EN 50463-2 - railway applications – energy measurement on board trains – part 2: Energy measuring"," CEI, Standard, May 2018.

[4] H. Duzkaya, S. S. Tezcan, A. Ocak, and O. Kilic, "The design and prototype production of a low-power voltage sensor with a resistive divider," in *2024 8th International Symposium on Multidisciplinary Studies and Innovative Technologies (ISMSIT)*, 2024, pp. 1–5.

[5] "IEC 61869-103 - Instrument Transformers - part 103: The use of instrument transformers for power quality measurement." IEC, Technical report, Apr. 2012.

[6] W.-Z. Zong, Y. Li, Y.-C. Cheng, C.-Y. Zhang, Y. Xue, and G.-G. Li, "The design of a wide-band high-voltage divider," in *2010 International Conference on Power System Technology*, 2010, pp. 1–5.

[7] S. Xie, P. Shu, W. Ding, Z. Mu, Z. Wan, and H. Wang, "Development of the 10 kv wideband combined resistance-capacitance voltage divider unit," in *2020 IEEE International Conference on High Voltage Engineering and Application (ICHVE)*, 2020, pp. 1–4.

[8] G. Crotti, D. Giordano, and A. Sardi, "Development of a rc medium voltage divider for on-site use," in *CPEM 2010*, 2010, pp. 655–656.

[9] D. Giordano, G. Crotti, and A. Sardi, "Development and use of a medium voltage rc divider for on-site calibration," in *2011 IEEE International Workshop on Applied Measurements for Power Systems (AMPS)*, 2011, pp. 53–57.